

The Lherz spinel lherzolite: Refertilized rather than pristine mantle

V. Le Roux ^{a,*}, J.-L. Bodinier ^a, A. Tommasi ^a, O. Alard ^a,
J.-M. Dautria ^a, A. Vauchez ^a, A.J.V. Riches ^b

^a *Géosciences Montpellier, Université Montpellier II, CNRS, Place Eugène Bataillon 34095 Montpellier cedex 5, France*

^b *Department of Earth Sciences, The Open University, Walton Hall, Milton Keynes, MK7 6AA, United Kingdom*

Received 18 December 2006; received in revised form 14 May 2007; accepted 14 May 2007

Available online 24 May 2007

Editor: C.P. Jaupart

Abstract

Differentiation of the Earth's mantle and formation of continental and oceanic crust occur principally through partial melting and extraction of basaltic melt. Among the mantle rocks occurring at the Earth's surface, as tectonically-emplaced massifs, abyssal peridotites or xenoliths, the harzburgites (<5% clinopyroxene) are widely considered as refractory mantle residues left after extraction of a basaltic component. In contrast, the most fertile lherzolites (15% clinopyroxene) are generally regarded as pristine mantle, only weakly affected by partial melting. In this paper we present new convergent structural and geochemical data from the Lherz massif, the type-locality of lherzolite, indicating that the lherzolites from Lherz do not represent pristine mantle. Detailed structural mapping clearly shows that the lherzolites are secondary rocks formed at the expense of the harzburgites. Variations of major, minor and trace elements through the harzburgite–lherzolite contacts indicate that the lherzolites were formed through a refertilization process involving interaction of refractory, lithospheric mantle with upwelling asthenospheric partial melts. Combined with previously published indications of refertilization in orogenic peridotites, our new observations in Lherz suggest that most lherzolite massifs represent secondary (refertilized) rather than pristine mantle. Together with geochemical data on mantle xenoliths, this indicates that melt transport and melt-rock reaction play a key role on the rejuvenation and erosion of the lithospheric mantle.

© 2007 Elsevier B.V. All rights reserved.

Keywords: Lherz; refertilization; melt-rock reaction; erosion of the lithospheric mantle

1. Introduction

Chemical variations observed in mantle rocks are classically ascribed to variable degrees of partial melting and melt extraction: the most fertile lherzolites (15% clinopyroxene) are interpreted as pristine mantle only weakly affected by partial melting whereas harzburgites

(<5% clinopyroxene) record high degrees of melt extraction (Frey et al., 1985; Bodinier, 1988). Together with chondritic meteorites, these fertile lherzolites were used to infer the composition of the Earth's primitive mantle (McDonough and Sun, 1995). In this scheme, tectonically-emplaced peridotite massifs equilibrated in the plagioclase (Lanzo, Italy (Boudier and Nicolas, 1977; Bodinier, 1988); Othris, Greece (Menzies and Allen, 1974); Horoman, Japan (Frey et al., 1991)), spinel (Ronda, Spain (Dickey, 1970; Frey et al., 1985); Lherz, France (Bodinier et al., 1988); Ivrea, Italy (Hartmann and Wedephol, 1993)) and garnet fields (Western Gneiss

* Corresponding author.

E-mail addresses: le-roux@gm.univ-montp2.fr (V. Le Roux), bodin@gm.univ-montp2.fr (J.-L. Bodinier), deia@gm.univ-montp2.fr (A. Tommasi).

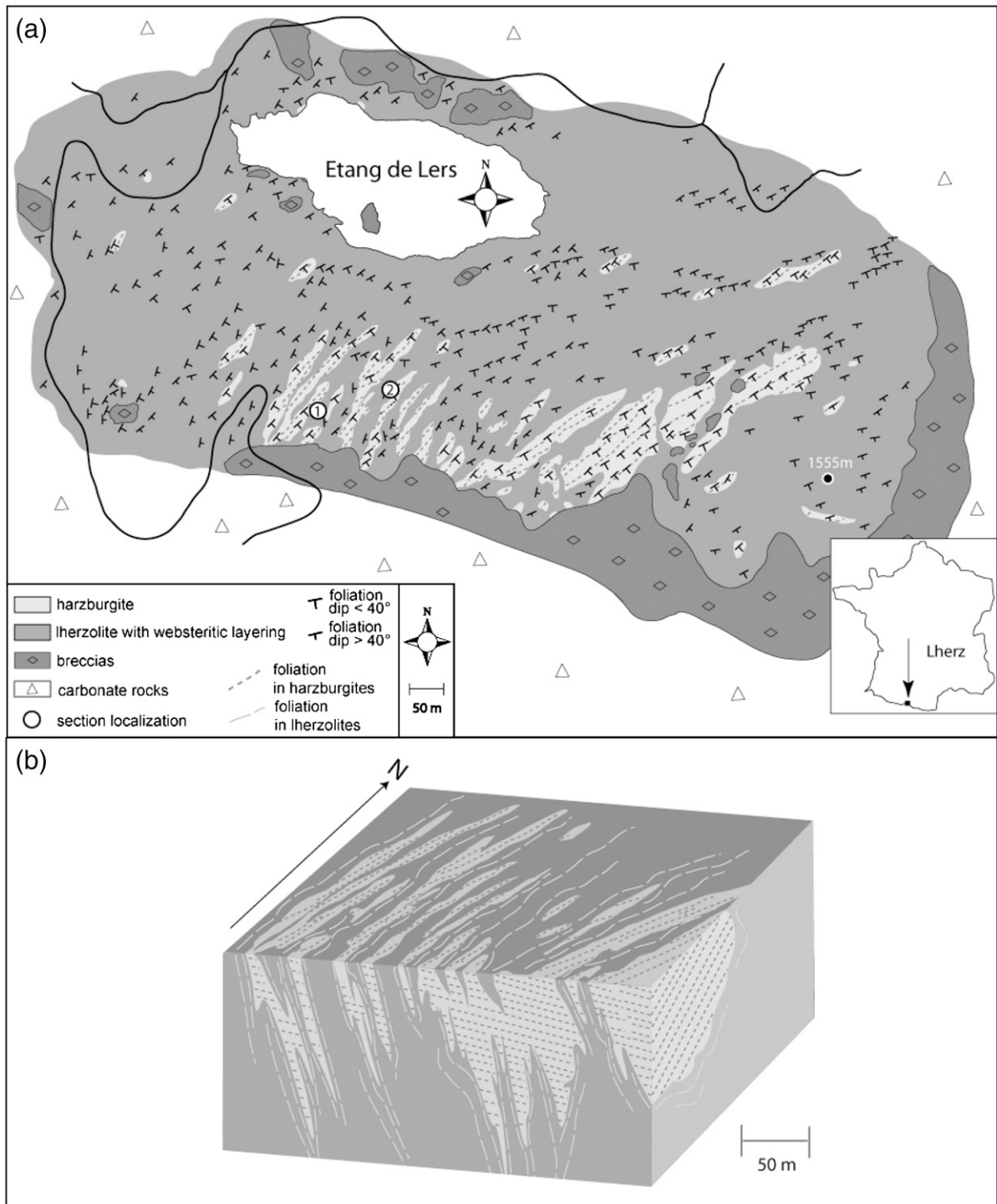


Fig. 1. (a) Geological map of the Lherz peridotite massif showing anastomosed fertile lherzolites enclosing irregularly-shaped refractory harzburgite bodies. Foliation in harzburgites shows a constant N40–N60 orientation with a gentle southward dip, while lherzolite foliation and websterite layering show variable directions and a steep southward dip. Right insert: localization of the massif. (b) 3-D bloc diagram of the upper part of the massif made after the dips of websterite layering at the contact.

Region, Norway (Carswell, 1968)) were widely considered as residual mantle containing sparse remnants of pristine material. However, an increasing set of observations shows that lherzolites may also form by combined processes of partial melting and igneous refertilization. Plagioclase lherzolites, in particular, are interpreted as products of impregnation of previously depleted peridotites by percolating melts (Nicolas and Dupuy, 1984; Rampone et al., 1994; Rampone et al., 1997; Saal et al., 2001; Piccardo et al., 2004). Müntener et al. (2004) have ascribed the formation of plagioclase peridotites in western Alps and Apennines to a reaction between extending lithosphere from embryonic ocean basins and upwelling asthenospheric melts. Spinel lherzolites from the Ronda Massif (S Spain) have also been ascribed to refertilization of subcontinental lithosphere (Van der Wal and Bodinier, 1996; Lenoir et al., 2001). In Ronda, this process was coupled with thermal erosion and extensive melting of deeper lithospheric levels (Garrido and Bodinier, 1999; Lenoir et al., 2001). Finally, Beyer et al. (2006) recently interpreted garnet peridotites and pyroxenites from the Western Gneiss Region (Norway) as formed by refertilization of a dunitic Archean lithospheric mantle.

The Lherz Massif in the Central Pyrenees, France, which is the type-locality of lherzolite, shows a decametric-scale intermingling of highly refractory harzburgites and fertile spinel lherzolites. This km-scale orogenic peridotite is therefore a natural laboratory to study the relations between depleted and fertile mantle rocks. We present here a detailed structural mapping of this massif combined with petrophysical and geochemical (major and trace elements) analyses performed along two distinct, 7–8 m-long sections across harzburgite–lherzolite contacts (11 harzburgites and 8 lherzolites). Additionally, 2 harzburgites and 2 lherzolites collected away from the contacts (>20 m) were studied for comparison. Our results provide a unique set of convergent structural and geochemical arguments indicating that the Lherz spinel lherzolites were formed by a refertilization reaction between a refractory harzburgitic–dunitic protolith and ascending basaltic melts. Combined with previous studies on worldwide mantle rocks, these results allow us to discuss the extent of the refertilization process and its implications for the rejuvenation and erosion of the lithospheric mantle.

2. Geological background

The Pyrenean orogenic peridotites comprise about 40 distinct ultramafic bodies mainly composed of layered spinel lherzolites, with dimensions varying from a few

m² to 1 km² in Lherz (Fabries et al., 1991). Most massifs are spatially associated with crustal granulites (Azambre and Ravier, 1978; Vielzeuf and Kornprobst, 1984) and are embedded within carbonate rocks of Jurassic to Aptian age affected by a low pressure–high temperature metamorphism (the ‘North Pyrenean Metamorphic Zone’) (Montigny et al., 1986; Golberg and Leyreloup, 1990). Exhumation of mantle rocks is generally ascribed to transcurrent movement of the Iberian plate relative to Europe in the mid-Cretaceous, which resulted in crustal thinning associated with successive opening and closing of elongated, asymmetrical pull-apart basins (Choukroune and Mattauer, 1978; Debros, 1987).

The Lherz massif is predominantly composed of spinel lherzolites which are intermingled with metric to decametric bodies of highly refractory harzburgites in the upper part of the massif (Fig. 1). The lherzolites contain numerous cm- to 10 cm-scale spinel–websterite layers and some thicker (10–50 cm) tabular garnet pyroxenites. The harzburgites often contain mm- to cm-thick websterite layers near the contact with lherzolites. Shortly before the exhumation, the massif was cross-cut by a late generation of amphibole pyroxenite dykes

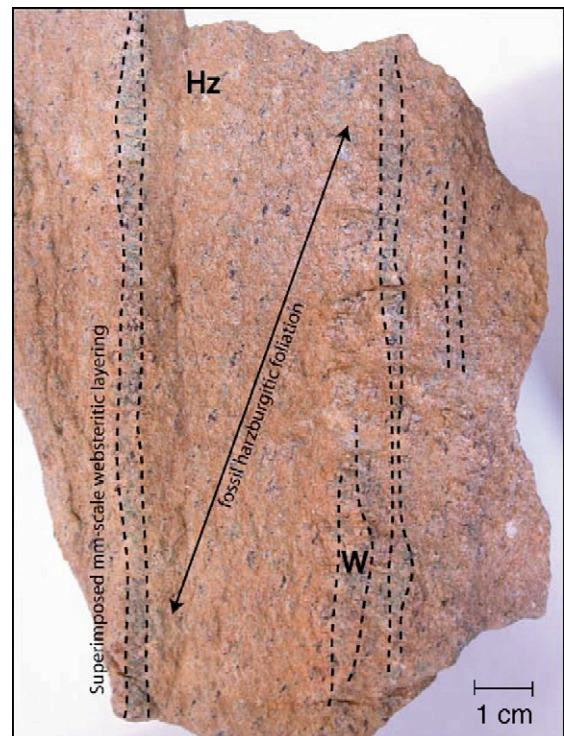


Fig. 2. Print of the fossil harzburgitic foliation in harzburgites (Hz) close to the contact, cross-cut by a latter mm-scale websteritic layering (W) related to the refertilization. The thin layering superimposed to the harzburgitic foliation initiates the development of cm-scale websteritic veins.

considered to represent trans-lithospheric melt conduits for Cretaceous alkaline magmatism in Pyrenees (Conqu er , 1971; Montigny et al., 1986; Bodinier et al., 1987; V etil et al., 1988). Narrow metasomatized dyke wall rocks and hornblendites veins record limited melt infiltration in host peridotites (Bodinier et al., 1990; Bodinier et al., 2004). The final emplacement of the peridotites is marked by extensive brecciation in the outer rim of the Lherz body and in the host limestones.

3. Structural and microstructural data

Previous structural maps of the Lherz Massif showed the harzburgites as elongated strips parallel to the high-temperature foliation of the lherzolites. However the present detailed mapping reveals that the harzburgite bodies form elongated, but irregularly-shaped bodies within

anastomosed lherzolites (Fig. 1). All harzburgites, even those forming small isolated bodies, show a penetrative shallowly-dipping foliation with a constant N40–60 E orientation which is marked by elongated spinels and olivine porphyroclasts. The contact with the lherzolites is often sharp and steep, and underlined by a cm-scale websteritic layering. Near the contact (<1 m) with harzburgites, the lherzolites are generally coarse-grained and show a weak foliation. This foliation is variable in orientation (N10 to N80), steeply dipping towards the east or south, and generally oblique on the harzburgite foliation (Figs. 1 and 2). Both layering and foliation in the lherzolites tend to wrap the contact with the harzburgite bodies. Away from the contact, fertile lherzolites display a steeply dipping foliation, dominantly N40–N80, marked by alignment of spinel aggregates that parallels the cm-scale websteritic layering.

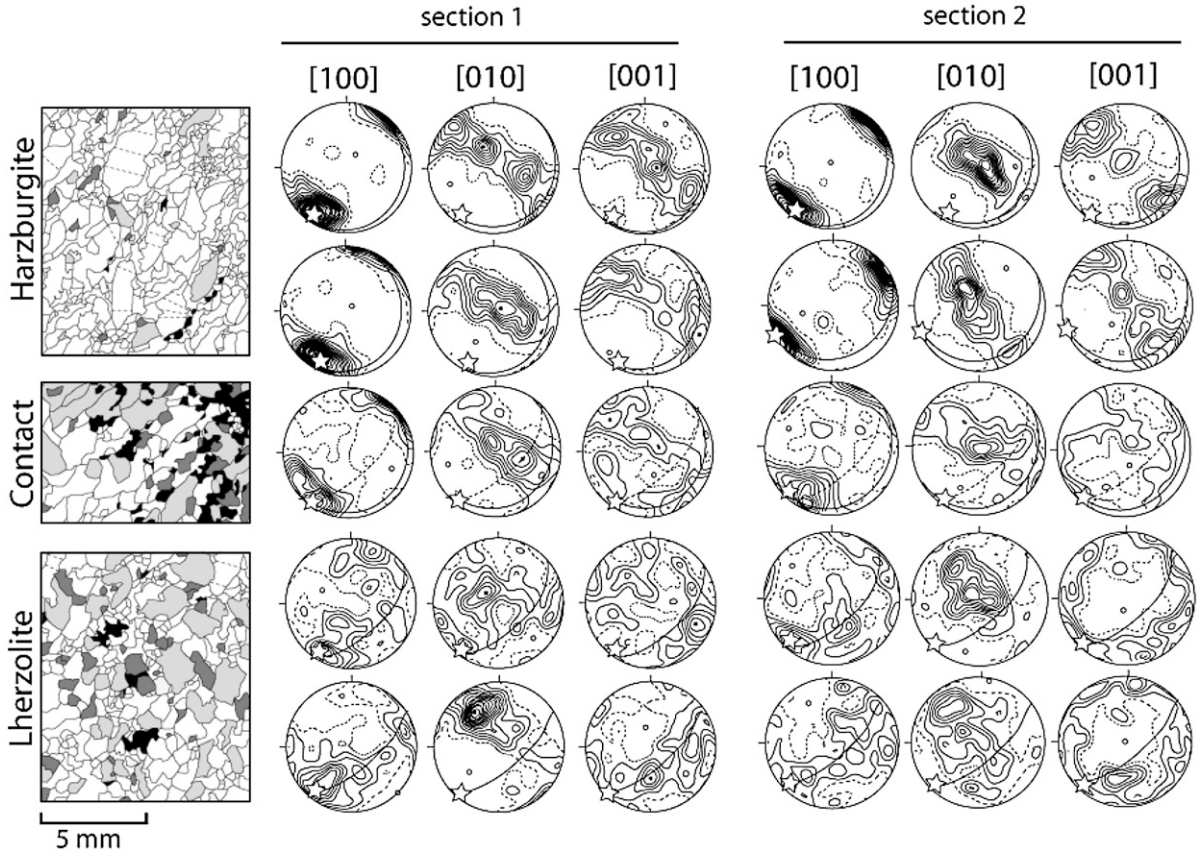


Fig. 3. Change in microstructure (left), from high-temperature porphyroclastic to coarse-granular, and associated weakening of olivine crystallographic preferred orientations (right) across two harzburgite–lherzolite contacts (Sections 1 and 2). The presented CPO are representative of all measured CPO through the contacts. Microstructures are from samples collected within 1 m from the contact, marked by cm-scale websterite banding. Microstructures were hand-drawn from thin sections; white: olivine, dashed lines mark subgrain boundaries; light grey: enstatite, dark grey: clinopyroxene; black: spinel. Olivine CPO are presented as lower-hemisphere equal area stereographic projections in a geographic reference frame (top to North); >130 individual grain measurements; contours at 0.5 multiple of a uniform distribution intervals. Solid lines: foliation; dashed lines: websterite layering; empty stars: lineation.

Table 1

Whole-rock major- and trace-element contents, and modal compositions, of Lherz peridotites collected along two sections across harzburgite–lherzolite contacts and in distal peridotites

Section 1													
Sample	05LD1	05LD4	05LA2	05LA1	05LA16	05LA9	05LA12	05LA3	05LA4	05LA5	05LA6	05LA8	05LA15
	Distal harz.	Distal harz.	harz.	harz.	harz.	harz.	harz.	harz.	harz.	lherz.	lherz.	lherz.	lherz.
Distance from contact	>20 m	>20 m	4.5 m	3.5 m	1 m	1 m	10 cm	10 cm	5 cm	1.5 m	3 m	5 m	5 m
SiO ₂ (wt.%)	39.2	42.1	44.7	43.1	42.3	41.9	42.2	41.4	41.5	46.2	44.8	45.4	46.9
Al ₂ O ₃	0.170	0.920	1.87	0.880	0.640	0.980	2.46	1.26	0.700	4.97	3.01	3.53	4.03
Cr ₂ O ₃	0.094	0.437	0.796	0.293	0.304	0.299	1.06	0.596	0.230	0.463	0.341	0.394	0.386
FeO	7.82	7.59	7.31	7.43	7.94	6.85	7.80	7.85	7.84	7.43	8.63	8.26	7.29
MgO	45.5	43.1	41.9	43.9	44.4	40.8	40.5	42.0	43.0	34.9	38.6	37.2	36.4
CaO	0.280	0.610	0.730	0.500	0.320	0.580	1.90	0.470	0.440	4.70	2.20	3.42	3.31
MnO	0.120	0.120	0.130	0.120	0.120	0.120	0.120	0.120	0.120	0.130	0.140	0.140	0.130
NiO	0.370	0.313	0.263	0.296	0.290	0.283	0.267	0.297	0.299	0.232	0.246	0.243	0.209
Na ₂ O	0.050	0.060	0.090	0.070	0.080	0.060	0.160	0.070	0.070	0.360	0.200	0.290	0.260
TiO ₂	0.030	0.020	0.040	0.060	0.050	0.030	0.060	0.050	0.040	0.200	0.100	0.140	0.160
LOI	6.44	4.46	2.93	3.85	3.48	7.83	3.41	5.95	5.73	0.480	1.33	1.04	0.820
Total	100.1	99.6	100.8	100.5	99.9	99.8	100.0	100.0	99.9	100.0	99.6	100.1	99.8
Modal composition													
Ol%	94.0	79.5	66.8	76.9	79.5	71.4	69.1	75.3	79.6	45.5	57.3	54.4	47.1
Opx%	4.6	16.8	27.7	20.3	18.4	25.7	16.7	20.8	17.9	28.5	29.5	28.4	34.4
Cpx%	1.2	2.4	3.1	2.1	1.5	2.3	10.7	2.2	1.9	22.7	10.9	15.2	15.7
Sp1%	0.2	1.2	2.5	0.7	0.6	0.6	3.5	1.7	0.6	3.3	2.3	2.0	2.8
Mg#	92.0	91.8	91.9	92.1	91.7	92.2	91.1	91.4	91.6	90.3	89.8	89.9	90.8
Section 2													
Sample	04LH13	04LH12	04LH14	04LH11	04LH08	04LH1815	04LH07	04LH04	05L3	05LE3			
	harz.	harz.	harz.	harz.	lherz.	lherz.	lherz.	lherz.	lherz.	lherz.	lherz.	lherz.	
Distance from contact	2 m	1.5 m	1.2 m	1 m	10 cm	50 cm	80 cm	1.5 m	>20 m	>20 m			
SiO ₂ (wt.%)	41.3	41.5	41.5	41.9	43.9	43.8	40.9	44.3	44.1	44.4			
Al ₂ O ₃	0.439	0.450	0.444	0.539	2.10	3.40	1.87	3.15	2.99	2.95			
Cr ₂ O ₃	0.287	0.252	0.223	0.274	0.461	0.356	0.547	0.377	0.342	0.353			
FeO	7.70	7.71	7.88	7.87	7.65	7.57	7.72	7.87	7.91	7.79			
MgO	43.8	43.4	43.8	44.2	41.9	38.3	40.2	39.3	38.7	39.6			
CaO	0.358	0.351	0.319	0.382	2.18	3.26	2.01	2.66	2.69	2.46			
MnO	0.118	0.118	0.119	0.121	0.125	0.129	0.124	0.132	0.130	0.130			
NiO	0.296	0.298	0.299	0.292	0.260	0.243	0.284	0.240	0.260	0.251			
Na ₂ O	0.048	0.040	0.045	0.058	0.219	0.290	0.185	0.216	0.210	0.200			
TiO ₂	0.010	0.012	0.016	0.017	0.124	0.153	0.082	0.131	0.130	0.120			
LOI	4.81	5.23	4.49	4.10	0.680	0.350	1.23	1.75	2.62	1.43			
Total	99.1	99.4	99.1	99.7	99.7	97.9	95.1	100.1	100.0	99.7			
Modal composition													
Ol%	82.0	82.9	84.1	80.4	59.9	72.6	61.6	68.8	63.6	60.9			
Opx%	15.9	15.3	14.1	17.6	26.3	16.2	20.8	19.9	22.7	25.6			
Cpx%	1.5	1.4	1.4	1.5	11.7	9.3	14.9	9.7	12.0	11.3			
Sp1%	0.6	0.4	0.4	0.5	2.1	1.9	2.7	1.6	1.7	2.2			
Mg#	91.8	91.8	91.7	91.8	90.8	91.2	90.9	91.6	90.6	91.0			

harz. = harzburgite; harz.* = harzburgite with thin (~mm) websterite layers; lherz. = lherzolite. LOI = loss on ignition; Mg# = Mg/Mg + Fe cationic ratio.

At the thin-section scale, harzburgites display a porphyroclastic microstructure, characteristic of deformation by dislocation creep (Fig. 3). Foliation and

lineation are marked by elongated spinels and olivine porphyroclasts with curvilinear grain boundaries, undulose extinction, and closely-spaced (100) subgrain

Table 2

Compositional ranges in major and minor elements of olivine (Ol), orthopyroxene (Opx), clinopyroxene (Cpx) and spinel (Spl) for harzburgites and lherzolites, and ranges of Mg# in olivine (=Mg/Mg+Fe cationic ratio) and Cr# in spinel (=Cr/Cr+Al cationic ratio)

Elements	Harzburgites				Lherzolites			
	Ol	Opx	Cpx	Spl	Ol	Opx	Cpx	Spl
SiO ₂ (wt.%)	40.7–41.8	56.5–57.5	53.5–54.4	0.074–0.195	40.6–41.4	54.8–57.2	51.7–52.8	0.100–0.145
Al ₂ O ₃	–	1.65–2.81	2.48–5.06	26.1–13.2	–	1.9–4.43	5.99–7.45	46.4–61.3
Cr ₂ O ₃	–	0.331–0.562	0.937–1.79	26.1–43.2	–	1.9–1.43	5.99–7.45	46.4–61.3
FeO	8.45–9.09	5.51–6.17	1.84–2.10	13.7–19.6	9.13–10.75	6.11–6.86	1.99–2.37	11.1–14.6
MgO	48.7–49.3	33.7–34.3	14.4–16.3	11.9–16.8	47.3–49.2	31.3–34.0	13.7–14.4	16.5–20.0
CaO	0.008–0.017	0.331–0.505	20.6–23.2	–	0.006–0.022	0.282–1.324	20.3–21.5	–
MnO	0.119–0.141	0.133–0.175	0.066–0.088	0.182–0.316	0.126–0.155	0.146–0.164	0.065–0.065	0.227–0.462
NiO	0.416–0.436	0.069–0.090	0.026–0.075	0.074–0.198	0.375–0.450	0.049–0.089	0.028–0.065	0.227–0.462
Na ₂ O	–	0.021–0.049	0.705–2.19	–	–	0.023–0.193	0.550–0.772	0.025–0.083
TiO ₂	–	0.014–0.098	0.051–0.321	0.018–0.172	–	0.103–0.193	0.550–0.772	0.025–0.083
Mg#	90.5–91.5				89.0–89.9			
Cr#				0.28–0.41				0.069–0.104

boundaries. Orthopyroxenes, as well as small clinopyroxenes (<1 mm), show irregular shapes and undulose extinction. Close to the contact, websterites and Cpx-poor lherzolites have coarser, more equant grains, but intracrystalline deformation features are still observed in olivine crystals. Spinel is interstitial and display no shape-preferred orientation. Farther from the contact, lherzolites display large (2–4 mm), equant clino- and orthopyroxenes. Elongate olivine porphyroclasts show a strong undulose extinction. Alignment of interstitial, holly-leaf spinels defines a clear lineation and foliation.

Crystallographic orientations (Fig. 3) were measured by indexation of Electron Back Scattered Diffraction

(EBSD) patterns using the SEM–EBSD system of Geosciences Montpellier (France). Measurements were performed manually (i.e. indexing of every crystal was verified by the operator) on grain by grain basis along 2 mm-spacing profiles parallel to the long axis of the thin section. The change in microstructure is associated with a variation in both orientation and strength of olivine crystal-preferred orientations (CPO). Harzburgites exhibit a strong olivine CPO, characterized by alignment of [100] axes close to the lineation and a girdle distribution of [010] and [001] with a maximum of [010] normal to the foliation.

At the contact, olivine CPO in the lherzolites is weaker but the orientation of the 3 maxima is preserved. In the

Table 3

REE compositions of clinopyroxene in four representative peridotites: a harzburgite and a lherzolite distal from harzburgite–lherzolite contacts, and the same rock types adjacent to a contact (Section 2 in Table 1)

Sample	05LD4			05LH11					04LH8						05LE3		
	Harzburgite			Harzburgite					Lherzolite						Lherzolite		
Distance from contact	>20 m			95 cm					10 cm						>20 m		
	cpx1	cpx2	cpx3	cpx1	cpx2	cpx3	cpx4	cpx5	cpx1	cpx2	cpx3	cpx4	cpx5	cpx6	cpx1	cpx2	cpx3
La (ppm)	0.857	0.584	0.676	7.81	7.59	7.18	5.78	6.58	1.74	1.59	1.57	1.39	1.63	1.64	0.933	0.918	0.893
Ce	1.70	1.19	1.75	14.4	13.9	14.2	11.7	12.6	5.99	5.63	5.47	5.19	5.59	5.66	3.69	3.50	3.33
Pr	0.241	0.180	0.239	1.51	1.45	1.48	1.29	1.34	1.23	1.16	1.11	1.09	1.13	1.11	0.661	0.634	0.625
Nd	1.11	1.16	1.37	5.83	5.70	5.73	5.07	5.26	7.87	7.30	6.94	6.94	7.25	7.14	3.96	3.91	3.93
Sm	0.340	0.337	0.388	1.32	1.37	1.34	1.22	1.29	2.85	2.73	2.61	2.62	2.72	2.71	1.69	1.54	1.70
Eu	0.103	0.103	0.107	0.458	0.466	0.465	0.434	0.458	1.08	1.06	1.01	1.02	1.03	1.03	0.726	0.674	0.700
Gd	0.369	0.365	0.407	1.47	1.52	1.50	1.45	1.54	3.77	3.51	3.35	3.28	3.50	3.55	2.41	2.56	2.44
Tb	0.050	0.054	0.058	0.245	0.246	0.247	0.448	0.249	0.613	0.560	0.541	0.525	0.560	0.558	0.433	0.451	0.466
Dy	0.353	0.341	0.369	1.74	1.71	1.65	1.76	1.82	3.97	3.69	3.72	3.61	3.79	3.72	3.33	3.44	3.53
Ho	0.076	0.075	0.0722	0.373	0.349	0.351	0.389	0.383	0.795	0.719	0.708	0.703	0.724	0.722	0.674	0.753	0.753
Er	0.259	0.259	0.243	1.09	1.05	1.04	1.23	1.14	2.15	1.96	1.96	1.93	1.94	1.99	2.16	2.30	2.32
Yb	0.409	0.403	0.295	1.16	1.07	1.04	1.37	1.21	1.79	1.76	1.72	1.75	1.76	1.77	2.15	2.24	2.18
Lu	0.063	0.067	0.058	0.171	0.155	0.163	0.208	0.180	0.251	0.244	0.248	0.247	0.234	0.254	0.279	0.304	0.302

lherzolites close to the contact, the weakening of the CPO is stronger, with a strong dispersion of [100] parallel to the layering but the orientation of [010] and [001] maxima is similar to the one in the harzburgites. Farther the contact, [010] axes are reoriented and the maximum concentration is normal to the lherzolite foliation.

4. Geochemical data

Major elements, Ti, Cr and Ni in whole rocks were analyzed by X-ray fluorescence at Geosciences Laboratories (Canada) and Open University (UK). Major and minor elements in olivine, orthopyroxene, clinopyroxene and spinel were analyzed by electron probe at Microsonde Sud facility, Montpellier (France), and Rare Earth Elements (REE) in clinopyroxene by laser-ablation plasma-mass spectrometry (LA-ICP-MS) at Geosciences Montpellier. Whole-rock analyses are reported in Table 1, compositional ranges in major and minor elements of minerals in Table 2 and representative REE analyses of clinopyroxene in Table 3.

Modal compositions calculated by linear inversion of whole-rock and mineral compositions for major elements are given in Table 1. They range from 94% Ol, 4.6% Opx, 1.2% Cpx and <1% Spl in harzburgites to 62% Ol, 21% Opx, 15% Cpx and >2% Spl in lherzolites. Major and minor elements in whole rocks display a wide range of variation from highly refractory (e.g., 45.53 wt.% MgO and 0.17 wt.% Al_2O_3) to very fertile compositions (34.85 wt.% MgO and 4.97 wt.% Al_2O_3). Harzburgites collected in the vicinity of lherzolites (<5 m) are more fertile on average than more distal harzburgites. Their modal and major-element compositions partly overlap the composition of lherzolites (e.g., in the range 2–2.5 wt.% Al_2O_3 — Table 1; Fig. 4). This feature reflects the presence of mm-scale websterite layers that are abundant near the contact with lherzolites. This is the case, for instance, in sample 05LA12 which is lherzolitic in terms of major-element and modal composition (10.7% Cpx). However, this sample is distinguished from the “true” lherzolites from Lherz by lower Ti and much higher Cr contents (Fig. 4) and by mineral compositions typical of harzburgites (Table 2, Annex 1). It is therefore referred to as a harzburgite throughout this study.

Similar to the majority of mantle peridotite suites worldwide, the harzburgites and lherzolites from Lherz display chemical covariations such as decreasing MgO with increasing Al_2O_3 traditionally ascribed to partial melting (Fig. 4). A more detailed analysis shows however that harzburgites and lherzolites tend to define distinct covariation trends, notably for minor elements. For instance the lherzolites are distinguished by slightly

higher Ti contents at a given Al_2O_3 value (Fig. 4). On a Cr vs. Al_2O_3 diagram, the difference between the harzburgite and lherzolite trends is striking: while the harzburgites show a steep, steady positive correlation, the lherzolites display a curved trajectory trending towards a gentle, positive correlation in the most fertile

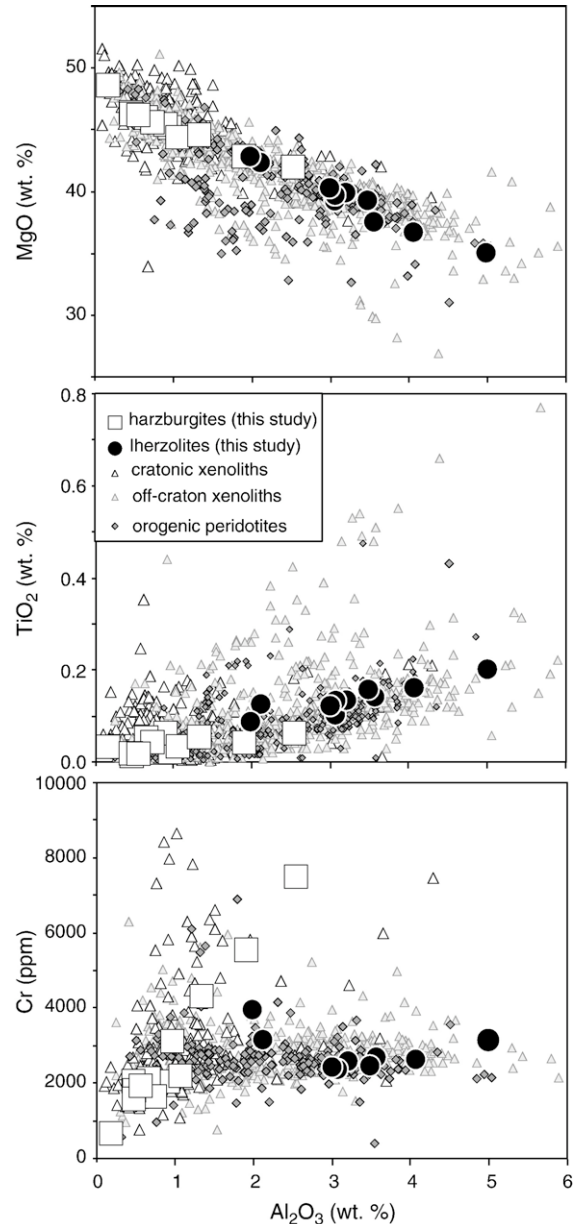


Fig. 4. MgO, TiO_2 and Cr vs. Al_2O_3 concentrations in whole-rock harzburgites and lherzolites from Lherz (Table 1) compared with literature data for mantle xenoliths and orogenic peridotites (Canil, 2004). Empty squares = harzburgites; full circles = lherzolites. The variations observed within a few meters across harzburgite–lherzolite contacts in Lherz encompass almost the whole range of mantle peridotites worldwide.

samples (Fig. 4). From their wide range of Cr contents (600 to 7400 ppm) and low Al_2O_3 values (<2.5%), the harzburgites resemble cratonic xenoliths, notably those equilibrated at shallow depth, in the stability field of spinel (Canil, 2004). Conversely, the lherzolites show a narrow range of Cr contents (2400–4000 ppm) and higher Al_2O_3 comparable to the composition of other orogenic peridotites and off-craton mantle xenoliths.

The existence of two different trends for Cr in covariation diagrams is a reflection of the markedly distinct Cr contents in minerals from harzburgites and lherzolites (Table 2). The Cr# number (=Cr/Cr+Al cationic ratio) of spinel, for instance, is in the range 0.28–0.41 in harzburgites compared with 0.069–0.104 in lherzolites. This bimodal distribution of mineral compositions is also observed for Mg# (=Mg/Mg+Fe cationic ratio) in olivine and minor elements such as Ti in pyroxenes. The forsterite value of olivine (Fo) is 0.905–0.915 in harzburgites, compared with 0.890–0.899 in lherzolites, and TiO_2 in clinopyroxene is 0.02–0.06 wt.% in harzburgites, compared with 0.12–0.20 wt.% in for lherzolites.

Rare earth elements (REE) in clinopyroxene display a wide range of concentrations and variable chondrite-

normalized REE patterns (Table 3; Fig. 5). In the core of the thickest harzburgite bodies (>10 m), clinopyroxene shows strongly depleted, U-shaped REE patterns. These REE patterns mimic the whole-rock patterns previously reported for harzburgites unrelated to pyroxenite dykes and lherzolites (Bodinier et al., 1988; Bodinier et al., 2004). In lherzolites away from contacts (>20 m), clinopyroxene displays the classic, N-MORB, REE pattern observed in orogenic lherzolites worldwide (McDonough and Frey, 1989). This pattern is relatively enriched in heavy REE but selectively depleted in light REE. Within a few meters from the contact, both lherzolite and harzburgite show more LREE-enriched clinopyroxenes than their distal counterparts. The variations observed in harzburgites are especially striking: the REE content of clinopyroxene increases by a factor of 5 (heavy REE) to 10 (light REE) from the core of the harzburgite bodies to the contacts.

5. Discussion

5.1. Structural relationships between harzburgitic protolith and secondary lherzolites

The constant orientation of the foliation and lineation in harzburgite bodies throughout the Lherz Massif (Fig. 1) strongly suggests that all harzburgites were once part of a single and continuous unit. This, together with the observation that the steeply dipping lherzolite foliation and websterite layering cross-cut the shallowly dipping harzburgite foliation, indicates that the deformation of the harzburgites predates the formation of the lherzolites and websterites. Such structural relationships between harzburgites and lherzolites, visible throughout the intermingled zone and at the massif-scale (Fig. 1), clearly indicate that the lherzolites are secondary rocks compared to harzburgites. The harzburgite bodies represent the remnants of a highly refractory mantle protolith largely replaced by the lherzolites.

Analysis of microstructures and olivine CPO suggest deformation of harzburgites by dislocation creep with activation of the high-temperature, low-stress (010) [100] slip system. The formation of the lherzolites and websterites modifies both the microstructure and the CPO of the harzburgitic protolith. However, while the change in microstructure, marked by grain growth, occurs at the contact, the re-orientation of the [100] and [010] axis of olivine, parallel to the lineation and perpendicular to the lherzolite foliation respectively, is only observed at some distance from the contact (>1–2 m). At the contact, lherzolites show larger and more equant grains and olivine CPO are quite similar to harzburgites,

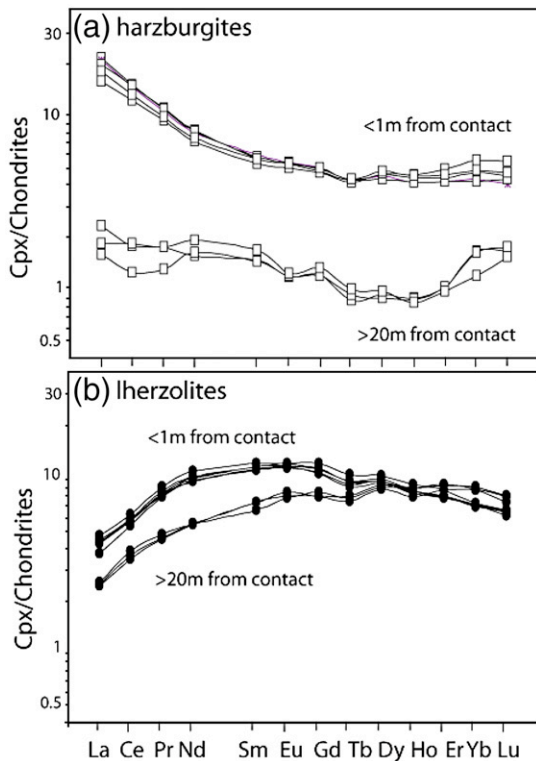


Fig. 5. Chondrite-normalized (Sun and McDonough, 1989) REE patterns of clinopyroxenes in four representative peridotites, including harzburgites and lherzolites, both distal and adjacent to a harzburgite–lherzolite contact (Table 2).

but weaker. The increase in grain size and the dispersion of the olivine CPO in lherzolites through harzburgite–lherzolite contacts may be due to static recrystallization and crystallization of new randomly-oriented olivine crystals during melt-rock reactions (Tommasi et al., 2004). The more pronounced growth of Opx and Cpx together with the increase in their modal proportions suggests that they represent the main crystallization products of the reaction. Far from the contact, olivine microstructures and CPO are consistent with the steeply-dipping foliations and sub-horizontal lineations observed at the macroscopic scale. These observations suggest that melt percolation and melt-rock reactions started at static conditions, leading to changes in modal composition, grain growth and dispersion of olivine CPO. This percolation produced an anastomosed lherzolite network in which the later deformation producing the steeply dipping foliations was localised.

Our structural observations preclude therefore the formation of the harzburgite–lherzolite intercalations by mechanical dispersion by small-scale convection at the base of the lithosphere (Bodinier and Godard, 2003), since this deformation would result in transposition of both harzburgites (lithospheric material) and lherzolites (asthenospheric material) foliations. The structural observations are on the other hand consistent with the formation of lherzolites by a near-solidus refertilization reaction between harzburgite and basaltic melts leading to precipitation of pyroxene, spinel, minor amphibole and sulphide phase, which started under static conditions and was followed by a deformation stage.

5.2. Formation of the lherzolites by refertilization reaction

Covariations of modal and major-element compositions in the Lherz peridotites are comparable to those observed in several suites of mantle rocks worldwide. These covariations were generally ascribed to variable degrees of partial melt extraction (Frey et al., 1985; Bodinier, 1988; Canil, 2004), although in most cases variable degrees of refertilization of a refractory protolith would also account for the observed modal and chemical trends (Beyer et al., 2006). In the case of Lherz, the partial melting model is precluded by structural observations that show that the harzburgite predate the lherzolites. Formation of harzburgite–lherzolite intercalations by variable degrees of melting is also ruled out by variations of minor and trace elements in peridotites and/or their constituent minerals.

Chromium, for instance, shows two features at odds with the partial melting model. First, although highly compatible during mantle melting (Liu and O'Neill,

2004), this element tends to be negatively correlated with MgO and positively correlated with Al_2O_3 (Fig. 4). Second, harzburgites and lherzolites form two different trends on Cr vs. major-element correlation diagrams, a feature that reflects the bimodal distribution of the Cr content in minerals, notably spinel. In contrast with melt extraction, refertilization of a refractory protolith involving precipitation of Cr- and Al-bearing minerals, mostly spinel and pyroxenes, can explain both the positive Cr vs. Al_2O_3 correlations and the existence of distinct Cr arrays for harzburgites and lherzolites (Fig. 6). In this model, the intersection of the harzburgite and lherzolite trends at low (<1%) Al_2O_3 content indicates the composition of the refractory protolith before refertilization. The lherzolite trend is interpreted as a linear mixing line between the depleted protolith composition and 30–60 wt.% of an aluminous websterite component (60% Opx, 34% Cpx, 6% Spl). Mineral compositions in the websterite are identical to those in lherzolites, as it is the case for thin (<10 cm) websterite layers in Lherz (Fabries et al., 1991) and other orogenic lherzolites (Shervais and Mukasa, 1991). The harzburgite trend is

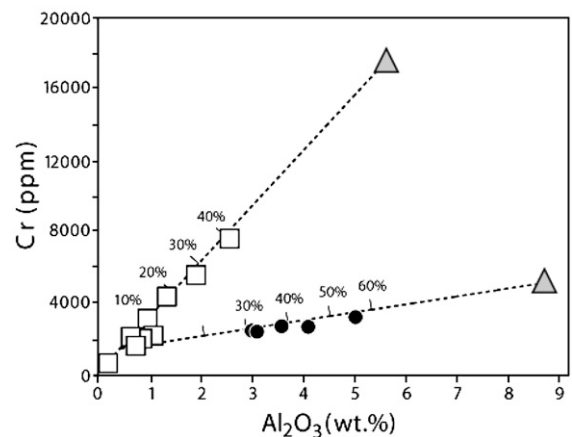


Fig. 6. Cr vs. Al_2O_3 diagram for the peridotites of Section 1 and distal samples (Table 1), emphasizing the two distinct covariation trends observed in lherzolites and harzburgites, respectively. The symbols for the samples are the same as in Fig. 4. The dashed lines represent mixing between a refractory harzburgite (intersection of the harzburgite and lherzolite trends) and variable proportions (in percent) of two distinct websterite components (grey triangles). The compositions of the websterite components were calculated from modal and mineral compositions. Modal compositions estimated by extrapolating those of the peridotites towards 0% olivine are roughly identical for harzburgites and lherzolites (60% Opx, 34% Cpx and 6% Sp). Websterite mineral compositions were measured in thin (<1 cm) websterite layers hosted by harzburgites and lherzolites. In both cases, the mineral compositions are similar in websterites and in their host peridotites, but they differ markedly between harzburgites and lherzolites. As a result, the two websterite components show distinct compositions, the one related to harzburgites being much more enriched in Cr than the one related to lherzolites.

defined by harzburgite samples collected within a few meters from the contact with lherzolites and containing thin (~mm) websterite seams (Section 1 in Table 1). These samples may be accounted for by mixing of the refractory protolith with 10–40 wt.% of a Cr-rich websterite component comparable to the harzburgites in terms of mineral compositions. These harzburgites were probably slightly refertilized by Cr-rich (harzburgite-buffered) small volume melts infiltrated beyond the main refertilization front represented by the harzburgite–lherzolite contact. The inferred variation in percolating melt composition, also reflected by bimodal Cr contents in minerals, may be explained by chromatographic fractionation of Cr due to cation exchange between the peridotite and the percolating melt (Navon and Stolper, 1987). The coincidence of the Cr chromatographic front with the harzburgite–lherzolite contact indicates a significant drop in the melt fraction across the reaction front as a result of partial melt consumption by the reaction (Bodinier et al., 2004).

Titanium differs from chromium in showing closely spaced, almost aligned covariation trends for harzburgites and lherzolites on the TiO_2 vs. Al_2O_3 diagram (Fig. 4). Hence the two arrays may be overlooked and viewed as a single correlation recording variable degrees of partial melting. However, the distribution of Ti in Cpx precludes this process. It is roughly constant in lherzolites and drops abruptly in harzburgites, whereas melting models predict a gradual decrease of Ti contents in both whole rocks and minerals (Fig. 7). When recalculated for near-solidus, high-temperature conditions (1250 °C), the bimodal distribution of Ti in Cpx is less pronounced but the discrepancy with the melting models remains significant. As shown in Fig. 7, the distribution of Ti can be successfully reproduced with a numerical simulation of refertilization involving a pyroxene- and spinel-forming reaction (Vernières et al., 1997). Based on the intersections of the harzburgite and lherzolites trends on Cr vs. modal and major-element composition diagrams (e.g., Fig 6), the protolith is assumed to be a highly refractory harzburgite (1.5% Cpx, 0.02 wt.% TiO_2). The Ti content of the infiltrated melt was derived from the composition of clinopyroxene in the most fertile lherzolite and Cpx/melt partition coefficients (Wood and Blundy, 2003). The results indicate constant Ti concentration in clinopyroxene of refertilized peridotites, which have their mineral compositions governed by incoming melt. Downstream of the Ti chromatographic front, Ti in Cpx rapidly decreases in the more refractory harzburgites, which mostly preserve the mineral compositions of the protolith.

Finally, REE enrichments observed at the harzburgite–lherzolite contacts also cannot be explained by partial

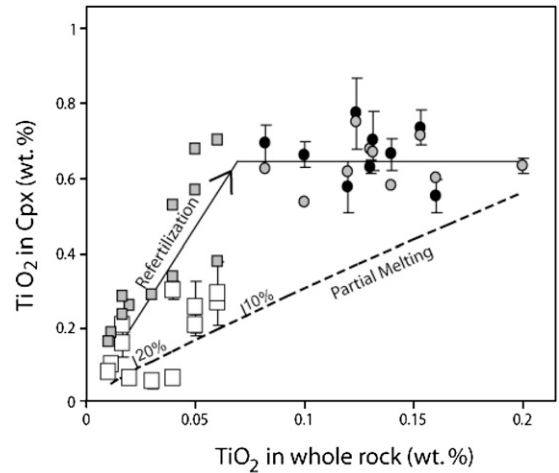


Fig. 7. TiO_2 concentrations in clinopyroxene vs. whole rocks for the harzburgites and lherzolites (same symbols as in Fig. 4). Error bars indicate the variation in Cpx composition at the sample scale. Grey symbols represent Cpx compositions recalculated for near-solidus temperature (1250 °C) using inter-mineral partition coefficients derived from Wood and Blundy (2003). Numerical models of TiO_2 variations during partial melting and magmatic refertilization are shown for comparison. For the melting model, we used the modal composition of the most fertile lherzolite, and its TiO_2 content in Cpx and whole rock, as the source composition. The melting reaction was taken from Walter et al. (1995) and the mineral/melt partition coefficients from Wood and Blundy (2003). The results reported here were calculated with the fractional melting model. However, changing the melting model (e.g. for batch or incremental melting) does not significantly modify the variation trend of TiO_2 in Cpx vs. whole rock. Magmatic refertilization was simulated with the Plate Model of Vernières et al. (1997) applied to the following melt-rock reaction: $f_i \cdot \text{melt}_i + x_{\text{ol}} \cdot \text{Ol} \rightarrow f_r \cdot \text{melt}_r + x_{\text{opx}} \cdot \text{Opx} + x_{\text{cpx}} \cdot \text{Cpx} + x_{\text{spl}} \cdot \text{Spl}$, where melt_i and melt_r stand for the infiltrated and residual melts, respectively, f_i and f_r for the corresponding melt mass fractions, x_{ol} for the mass fraction of dissolved olivine, and x_{opx} , x_{cpx} and x_{spl} for the mass fractions of crystallized Opx, Cpx, and Spl. Reaction parameters f_i , f_r , x_{ol} , x_{opx} , x_{cpx} and x_{spl} were adjusted to reproduce the modal variations and the Ti contents in Cpx and whole rocks. The protolith is a highly refractory harzburgite (83% Ol, 15% Opx, 1.5% Cpx, 0.5% Spl, 0.02 wt.% TiO_2 in whole rock and 0.05 wt.% TiO_2 in Cpx). The Ti content of the infiltrated melt ($\text{TiO}_2 = 2$ wt.%) was derived from the composition of clinopyroxene in the most fertile lherzolite and Cpx/melt partition coefficients (Wood and Blundy, 2003).

melting model and provide further evidence for the refertilization process. Strong enrichment of highly incompatible elements (HIE, including REE) at melt infiltration fronts is indeed predicted by theoretical modelling of melt-consuming reactions combined with melt transport (Vernières et al., 1997). This enrichment results from the segregation of HIE- and volatile-rich small melt fractions moving ahead of melt-consuming reaction fronts. This mechanism, also referred to as “percolative fractional crystallization” (Harte et al., 1993), was advocated to explain enriched HIE compositions in “cryptically”

metasomatized mantle xenoliths (Bedini et al., 1997) and in tens of cm-thick wall rocks of alkaline dykes in Lherz (Bodinier et al., 1990). In the case of the harzburgite–lherzolite contacts, the REE variation in harzburgite Cpx indicates that small melt fractions residual after the refertilization reaction migrated in the harzburgite protolith several meters (<20 m) ahead of the main reaction front. Behind the reaction front, clinopyroxene REE compositions in lherzolites reflect the initial melt composition, which is depleted in LREE relative to HREE (i.e., similar to N-MORB).

5.3. Refertilization and isotopic variations

A striking feature of Pyrenean and several other orogenic peridotites is the existence of correlations between Os–Sr–Nd radiogenic isotopes and peridotite fertility (Downes et al., 1991; Reisberg and Lorand, 1995; Bodinier and Godard, 2003). In the Pyrenees, the positive correlation between $^{187}\text{Os}/^{188}\text{Os}$ and Al_2O_3 has been ascribed to a ~ 2.5 Ga-old depletion event considered to record partial melting and stabilization of lithospheric mantle in the Archean (Reisberg and Lorand, 1995). However, this hypothesis does not account for the negative correlation of $^{87}\text{Sr}/^{86}\text{Sr}$ and the positive correlation of $^{143}\text{Nd}/^{144}\text{Nd}$ with Al_2O_3 . These covariations were ascribed either to selective percolation of enriched melts through the harzburgites (Downes et al., 1991) or to incomplete mixing of lithospheric strips (harzburgites) into asthenospheric material (lherzolites) during thermo-mechanical erosion of lithosphere by upwelling mantle (Bodinier and Godard, 2003). However, the first alternative implies unrealistically enriched melt compositions (Bodinier and Godard, 2003) and the second is denied by our structural observations. In contrast the refertilization process suggested in this paper provides a coherent explanation for the isotopic variations observed in Pyrenean peridotites. The correlations of $^{87}\text{Sr}/^{86}\text{Sr}$ and $^{143}\text{Nd}/^{144}\text{Nd}$ with Al_2O_3 indicate that the refractory protolith was isotopically enriched – due to radiogenic decay following ancient enrichment – while the percolating melt had a DMM (Depleted MORB Mantle) composition. The refertilization process may also account for the positive correlation between $^{187}\text{Os}/^{188}\text{Os}$ and Al_2O_3 , as previously suggested for the Horoman orogenic peridotite in Japan (Saal et al., 2001).

5.4. Refertilization fronts, a moving lithosphere–asthenosphere boundary?

In the light of our convergent structural and geochemical arguments we suggest that the Lherz massif is a

fossil lithosphere–asthenosphere boundary, where a >2 Ga-old (Reisberg and Lorand, 1995) and refractory lithospheric mantle, from which the harzburgites are the remnants, was infiltrated and reacted with asthenospheric melts. The irregularly-shaped lherzolite–harzburgite contacts represent therefore a convoluted melt–rock reaction front formed by coalescence of porous melt infiltration channels. All lithospheric structures and geochemical signatures were efficiently erased within a few meters across the front. The ubiquitous websterite layers record higher melt/rock ratios and suggest small-scale anisotropic variations in the melt flux. A possible origin for the websterite layering is refraction and channelling of percolating melts against the freezing horizon represented by eroded lithosphere (Sparks and Parmentier, 1991; Spiegelman, 1993; Rabinowicz and Ceuleneer, 2005). This hypothesis is consistent with the systematic parallelism of websterite layers and harzburgite–lherzolite contacts. It was already suggested for replacive websterite layers related to lithospheric thermal erosion in the Ronda peridotite (Garrido and Bodinier, 1999). The low equilibrium temperatures recorded by pyroxene compositions in the Lherz peridotites (Fabries et al., 1991) imply that thermal relaxation occurred between the refertilization episode and the emplacement of the massif in the crust, in the Cretaceous. Refertilization is thus probably related to the late-Variscan, post-collisional thermal event responsible for granulitic metamorphism in western Pyrenees (Pin and Vielzeuf, 1983), which has been interpreted as the result of the destabilization of the thickened orogenic lithosphere.

Is the refertilization process specific to Lherz? This is the first study showing convergent structural and geochemical data for extensive rejuvenation of refractory lithospheric mantle by refertilization. However, textural or chemical evidence for igneous refertilization has been reported from tectonically-emplaced plagioclase lherzolites in New Caledonia (Nicolas and Dupuy, 1984), western Alps (Rampone et al., 1994; Müntener et al., 2004), Horoman (Saal et al., 2001), and from Cpx-poor lherzolites at the base of the Oman ophiolite (Godard et al., 2000). Recently Beyer et al. (2006) suggested the transformation of highly refractory (dunitic) Archean lithospheric mantle via igneous refertilization, producing garnet peridotites and pyroxenites. An association between refertilization and lithospheric thinning was proposed for the orogenic lherzolites of Ronda and Lanzo (Lenoir et al., 2001; Müntener et al., 2004). The Ronda massif displays a narrow (<400 m) refertilization front which separates a spinel tectonite domain interpreted as an old lithospheric mantle and a granular

domain deeply modified by melting processes (Van der Wal and Bodinier, 1996; Lenoir et al., 2001). The refertilization front of the Lherz massif may have been associated with such a melting front below.

In the Cr vs. Al_2O_3 diagram, several suites of mantle rocks show variations comparable to those observed in the Lherz massif (Fig. 4). These variations are hardly consistent with partial melting and may suggest that the majority of lherzolites observed at the Earth surface record refertilization processes. The refertilization mechanism also provides a key to understanding the paradoxical association of LREE-enriched harzburgites with LREE-depleted lherzolites often observed in mantle xenoliths and in tectonically-emplaced peridotites (McDonough and Frey, 1989). Although recognized for at least two decades, this association, which is inconsistent with partial melting, was never given a satisfactory explanation.

6. Conclusions

The Lherz Massif, lithotype of the lherzolite, is an exceptional area for studying the structural and geochemical evolution of the sub-continental lithospheric mantle. Detailed structural mapping reveals that the Lherz spinel lherzolites are secondary rocks formed at the expense of harzburgites, which represent remnant bodies of an old (>2 Ga) and highly refractory protolith. Petrological and geochemical data show that the lherzolite–websterite suite has been formed by a near-solidus refertilization reaction involving crystallization of pyroxene and spinel, and dissolution of olivine. The irregular-shaped harzburgite–lherzolite contact thus materializes an anastomosed refertilization front formed by coalescence of melt infiltration channels. This evolution starts under static conditions but is followed by localisation of the deformation in the refertilized domains. Upwelling of basaltic partial melts through the lithospheric mantle was associated with the migration of an important refertilization front. At a larger-scale, the Ronda Massif (S Spain) also displays a refertilization front which is tightly linked to a partial melting domain below (Van der Wal and Bodinier, 1996; Lenoir et al., 2001). We can thus imagine that the refertilization front observed in the Lherz Massif also moved ahead of a melting front related to thermo-mechanical erosion of the lithosphere.

There is a growing body of evidence indicating that the chemical variations observed in tectonically-emplaced mantle rocks result from igneous refertilization superimposed onto previous depletion events. An important implication is that fertile lherzolites from peridotite massifs cannot be straightforwardly used to infer

primitive mantle compositions. In this perspective, it is logical to wonder whether the fertile mantle xenoliths represent refertilized or pristine mantle. Several authors have ascribed the chemical stratification of cratonic lithosphere and/or its temporal evolution to metasomatic refertilization (Lee and Rudnick, 1999; Kopylova and Russell, 2000; Griffin et al., 2003). In this scheme, fertile (predominantly lherzolitic), off-craton lithosphere may be viewed as the ultimate transformation of cratonic lithosphere after one or several cycles of igneous refertilization. Extensive refertilization in the Western Alps and Betic peridotites is intrinsically related to the lithospheric thinning processes that led to mantle exhumation (Lenoir et al., 2001; Piccardo et al., 2004; Müntener et al., 2004), which may suggest that large-scale refertilization is specific of tectonically-emplaced, orogenic peridotites. However, the Lherz massif illustrates a situation where refertilization and exhumation are related to distinct events, separated in time by thermal relaxation of the subcontinental mantle lithosphere. Several suites of spinel peridotite xenoliths compositionally comparable to the Lherz peridotites (i.e., formed of LREE-depleted lherzolites associated with subordinate, LREE-enriched harzburgites) might also record magmatic refertilization of a previously depleted lithospheric mantle.

Magmatic refertilization probably plays a key role in the rejuvenation and erosion of the lithospheric mantle. Seismological data suggest that the lithospheric mantle is strongly thinned in extensional environments (Bastow et al., 2005) and above mantle plumes (Li et al., 2004). Numerical models, however, predict that thermo-mechanical processes, like small-scale convective destabilization, only produce limited thinning (<30 km) (Thoraval et al., 2006), due to the strong temperature dependence of the viscosity and slow heat conduction in the lithospheric mantle. Refertilization of the lithospheric mantle by asthenospheric melts may reconcile these contrasting observations. Deformation experiments show that the presence of even a small fraction of basaltic melt results in a marked decrease of olivine-rich rocks strength (Hirth and Kohlstedt, 1995). Progression of the melt infiltration front producing the refertilization will therefore reduce the viscosity and favor the destabilization and removal of the lithospheric mantle.

Acknowledgements

This study was supported by the DyETI programme of INSU–CNRS and the Laboratoire de Tectonophysique, Montpellier. We thank Fred Frey for his comments on an earlier version of this paper, and Martin Menzies

and Cin-Ty Lee for their constructive reviews. We are grateful to Christophe Nevado and Doriane Delmas for providing high-quality thin sections, to Claude Merlet for his help with electron probe analyses, and to Olivier Bruguier and Simone Pourtales for their assistance during LA-ICP-MS analyses.

References

- Azambre, B., Ravier, J., 1978. Les écaïlles de gneiss du faciès granulitique du Port de Saleix et de la région de Lherz (Ariège). Nouveaux témoins du socle profond des Pyrénées. *Bull. Soc. Geol. Fr.* XX (3), 221–228.
- Bastow, I.D., Stuart, G.W., Kendall, J.-M., Ebinger, C.J., 2005. Upper-mantle seismic structure in a region of incipient continental breakup: northern Ethiopian rift. *Geophys. J. Int.* 162, 479–493. doi:10.1111/j.1365-246X.2005/02666.x.
- Bedini, R.M., Bodinier, J.-L., Dautria, J.-M., Morten, L., 1997. Evolution of LILE-enriched small melt fractions in the lithospheric mantle: a case study from the East African Rift. *Earth Planet. Sci. Lett.* 153, 67–83.
- Beyer, E.E., Griffin, W.L., O'Reilly, S.Y., 2006. Transformation of Archean lithospheric mantle by refertilization: evidence from exposed peridotites in the Western Gneiss Region, Norway. *J. Petrol.* 47 (8), 1611–1636.
- Bodinier, J.L., 1988. Geochemistry and petrogenesis of the Lanzo peridotite body, western Alps. *Tectonophysics* 149, 67–88.
- Bodinier, J.-L., Godard, M., 2003. Orogenic ophiolitic, and abyssal peridotites. In: Carlson, R.W. (Ed.), *Treatise on Geochemistry*, vol. 2. Elsevier, Amsterdam, pp. 103–170.
- Bodinier, J.-L., Fabries, J., Lorand, J.-P., Dostal, J.D., C., 1987. Geochemistry of amphibole pyroxenite veins from the Lherz and Freychinede ultramafic bodies (Ariege, French Pyrenees). *Bull. Mineral.* 110, 345–358.
- Bodinier, J.L., Dupuy, C., Dostal, J., 1988. Geochemistry and petrogenesis of Eastern Pyrenean peridotites. *Geochim. Cosmochim. Acta* 52, 2893–2907.
- Bodinier, J.L., Vasseur, G., Vernieres, J., Dupuy, C.F., J., 1990. Mechanisms of mantle metasomatism: geochemical evidence from the Lherz orogenic peridotite. *J. Petrol.* 31, 597–628.
- Bodinier, J.-L., Menzies, M.A., Shimizu, N., Frey, F.A., McPherson, E., 2004. Silicate, hydrous and carbonate metasomatism at Lherz, France: contemporaneous derivatives of silicate melt-harzburgite reaction. *J. Petrol.* 45 (2), 299–320. doi:10.1093/petrology/egg107.
- Boudier, F., Nicolas, A., 1977. Structural control on the partial melting of the Lanzo peridotite. *AGU Chapman Conf. Proc.*
- Canil, D., 2004. Mildly incompatible elements in peridotites and the origins of mantle lithosphere. *Lithos* 77, 375–393.
- Carswell, D.A., 1968. Picritic magma–residual dunite relationships in garnet peridotite at Kalskaret near Tafjord, South Norway. *Contrib. Mineral. Petrol.* 19 (2), 97–124.
- Choukroune, P., Mattauer, M., 1978. Tectonique des plaques et Pyrénées: sur le fonctionnement de la faille transformante nord-pyrénéenne; comparaison avec des modèles actuels. *Bull. Soc. Geol. Fr.* 20, 689–700.
- Conquéré, F., 1971. Les pyroxénites à amphibole et les amphibolites associées aux lherzolites du gisement de Lherz (Ariège, France): un exemple du rôle de l'eau au cours de la cristallisation fractionnée des liquides issus de la fusion partielle des lherzolites. *Contrib. Mineral. Petrol.* 33, 32–61.
- Debroas, E.J., 1987. Modèle de bassin triangulaire à l'intersection de décrochements divergents pour le fossé albo-cénomaniens de la Ballongue (zone nord-pyrénéenne, France). *Bull. Soc. Geol. Fr.* 8, 887–898.
- Dickey Jr, J.S., 1970. Partial fusion products in Alpine-type peridotites: Serrania de La Ronda and other examples. *Mineral Soc. Amer. Spec. Pap.* 3, 33–49.
- Downes, H., Bodinier, J.-L., Thirlwall, M.F., Lorand, J.-P., Fabries, J., 1991. REE and Sr–Nd isotopic geochemistry of Eastern Pyrenean peridotite massifs: sub-continental lithospheric mantle modified by continental magmatism. *J. Petrol. Special Lherzolite Issue*, 97–115.
- Fabries, J., Lorand, J.-P., Bodinier, J.-L., Dupuy, C., 1991. Evolution of the upper mantle beneath the Pyrenees: evidence from orogenic spinel lherzolite massifs. *J. Petrol. (Special Lherzolites Issue)* 55–76.
- Frey, F.A., Suen, C.J., Stockman, H.W., 1985. The Ronda high temperature peridotite: geochemistry and petrogenesis. *Geochim. Cosmochim. Acta* 49, 2469–2491.
- Frey, F., Shimizu, N., Leinbach, A., Obata, M., Takazawa, E., 1991. Compositional variations within the lower layered zone of the Horoman peridotites, Hokkaido, Japan: constraints on models for melt–solid segregation. In: Menzies, M.A., Dupuy, C., Nicolas, A. (Eds.), *Orogenic lherzolites and mantle processes*. Oxford University Press, Oxford.
- Garrido, C.J., Bodinier, J.-L., 1999. Diversity of mafic rocks in the Ronda peridotite: evidence for pervasive melt–rock reaction during heating of subcontinental lithosphere by upwelling asthenosphere. *J. Petrol.* 40 (5), 729–754.
- Godard, M., Jousselin, D., Bodinier, J.-L., 2000. Relationships between geochemistry and structure beneath a paleo-spreading centre: a study of the mantle section in the Oman Ophiolite. *Earth Planet. Sci. Lett.* 180, 133–148.
- Golberg, J.M., Leyreloup, A.F., 1990. High temperature–low pressure Cretaceous metamorphism related to crustal thinning (Eastern North Pyrenean Zone, France). *Contrib. Mineral. Petrol.* 104, 194–207.
- Griffin, W.L., O'Reilly, S.Y., Natapov, L.M., Ryan, C.G., 2003. The evolution of lithospheric mantle beneath the Kalahari Craton and its margins. *Lithos* 71, 215–242.
- Harte, B., Hunter, R.H., Kinny, P.D., 1993. Melt geometry, movement and crystallization, in relation to mantle dykes, veins and metasomatism. *Philosophical Transactions of the Royal Society of London* 342, 1–21.
- Hartmann, G., Wedephol, K.H., 1993. The composition of peridotites tectonites from the Ivrea complex (N-Italy) representing material at different stages of depletion. *Geochim. Cosmochim. Acta* 57, 1761–1782.
- Hirth, G., Kohlstedt, D.L., 1995. Experimental constraints on the dynamics of the partially molten upper mantle: deformation in the dislocation creep regime. *J. Geophys. Res.* 100 (B8), 15,441–15,449.
- Kopylova, M.G., Russell, J.K., 2000. Chemical stratification of cratonic lithosphere; constraints from the northern Slave Craton, Canada. *Earth Planet. Sci. Lett.* 181 (1–2), 71–87.
- Lee, C.-T., Rudnick, R.L., 1999. Compositionally stratified cratonic lithosphere: petrology and geochemistry of peridotite xenoliths from the Labait Volcano, Tanzania. In: Dawson, B.J.v., Gurney, J.J., Gurney, J.L., Pascoe, M.D., Richardson, S.R. (Eds.), *Proc. VIIIth International Kimberlite Conference*.
- Lenoir, X., Garrido, C.J., Bodinier, J.-L., Dautria, J.-M., Gervilla, F., 2001. The recrystallization front of the Ronda peridotite: evidence for melting and thermal erosion of subcontinental lithospheric mantle beneath the Alboran Basin. *J. Petrol.* 42, 141–158.
- Li, Y., Kind, R., Yuan, X., Wolber, I., Hanka, W., 2004. Rejuvenation of the lithosphere by the Hawaiian plume. *Nature* 427, 827–829.

- Liu, X., O'Neill, H.S.C., 2004. The effect of Cr_2O_3 on the partial melting of spinel lherzolite in the system $\text{CaO-MgO-Al}_2\text{O}_3\text{-SiO}_2\text{-Cr}_2\text{O}_3$ at 1.1 GPa. *J. Petrol.* 45 (11), 2261–2286.
- McDonough, W.F., Frey, F.A., 1989. Rare earth elements in upper mantle rocks. In: Lipin, B.R., McKay, G.A. (Eds.), *Geochemistry and Mineralogy of Rare Earth Elements*. Mineralogical Society of America, Washington DC, pp. 99–139.
- McDonough, W.F., Sun, S.-S., 1995. The composition of the Earth. *Chem. Geol.* 120, 223–253.
- Menzies, M.A., Allen, C., 1974. Plagioclase lherzolite–residual mantle relationships within two eastern Mediterranean ophiolites. *Contrib. Mineral. Petrol.* 45 (3), 197–213.
- Montigny, R., Azambre, B., Rossy, M., Thuizat, R., 1986. K–Ar study of Cretaceous magmatism and metamorphism of the Pyrenees: age and length of rotation of the Iberian Peninsula. *Tectonophysics* 129, 257–273.
- Müntener, O., Pettke, T., Desmurs, L., Meier, M., Schaltegger, U., 2004. Refertilization of mantle peridotite in embryonic ocean basins: trace element and Nd isotopic evidence and implications for crust–mantle relationships. *Earth Planet. Sci. Lett.* 221, 293–308. doi:10.1016/S0012-821X(04)00073-1.
- Navon, O., Stolper, E., 1987. Geochemical consequences of melt percolation: the upper mantle as a chromatographic column. *J. Geol.* 95, 285–307.
- Nicolas, A., Dupuy, C., 1984. Origin of ophiolitic and oceanic lherzolites. *Tectonophysics* 110, 177–187.
- Piccardo, G.B., Müntener, O., Zanetti, A., 2004. Alpine–Apennine ophiolitic peridotites: new concepts on their composition and evolution. *Ophioliti* 29 (1), 63–74.
- Pin, C., Vielzeuf, D., 1983. Granulites and related rocks in Variscan median Europe: a dualistic interpretation. *Tectonophysics* 93, 47–74.
- Rabinowicz, M., Ceuleneer, G., 2005. The effect of sloped isotherms on melt migration in the shallow mantle: a physical and numerical model based on observations in the Oman ophiolite. *Earth Planet. Sci. Lett.* 229, 231–246.
- Rampone, E., Piccardo, G.B., Vannucci, R., Bottazzi, P., Zanetti, A., 1994. Melt impregnation in ophiolitic peridotite: an ion microprobe study of clinopyroxene and plagioclase. *Min. Mag.* 58A, 756–757.
- Rampone, E., Piccardo, G.B., Vannucci, R., Bottazzi, P., 1997. Chemistry and origin of trapped melts in ophiolitic peridotites. *Geochim. Cosmochim. Acta* 61 (21), 4557–4569.
- Reisberg, L., Lorand, J.-P., 1995. Longevity of sub-continental mantle lithosphere from osmium isotope systematics in orogenic peridotite massifs. *Nature* 376, 159–162.
- Saal, A.E., Takazawa, E., Frey, F.A., Shimizu, N., Hart, S.R., 2001. Re–Os isotopes in the Horoman peridotite: evidence for refertilization? *J. Petrol.* 42 (1), 25–24.
- Shervais, J.W., Mukasa, S.B., The Balmuccia orogenic lherzolite massif, Italy, Menzies, M.A., Dupuy, C. and Nicolas, A., *Orogenic lherzolites and mantle processes*, Oxford University Press, Spc. vol. *J. Petrol.* (1991) 155–174 Oxford (U.K.).
- Sparks, D.W., Parmentier, E.M., 1991. Melt extraction from the mantle beneath spreading centres. *Earth Planet. Sci. Lett.* 105, 368–377.
- Spiegelman, M., 1993. Physics of melt extraction: theory, implications and applications. *Philosophical Transactions: Physical Sciences and Engineering* 342, 23–41.
- Sun, S.-S., McDonough, W.F., 1989. Chemical and isotopic systematics of oceanic basalts: implications for mantle composition and processes. In: Saunders, A.D., Norry, M.J. (Eds.), *Magmatism in the Ocean Basins*, vol. 42. *Geol. Soc. London*, pp. 313–345.
- Thoraval, C., Tommasi, A., Doin, M.-P., 2006. Plume–lithosphere interactions beneath a fast-moving plate. *Geophys. Res. Lett.* 33, L01301. doi:10.1029/2005GL024047.
- Tommasi, A., Godard, M., Coromina, G., Dautria, J.-M., Barszczus, H.G., 2004. Seismic anisotropy and compositionally induced velocity anomalies in the lithosphere above mantle plumes: a petrological and microstructural study of mantle xenoliths from French Polynesia. *Earth Planet. Sci. Lett.* 227, 539–556.
- Van der Wal, D., Bodinier, J.-L., 1996. Origin of the recrystallisation front in the Ronda peridotite by km-scale pervasive porous melt flow. *Contrib. Mineral. Petrol.* 122, 387–405.
- Vernières, J., Godard, M., Bodinier, J.-L., 1997. A plate model for the simulation of trace element fractionation during partial melting and magma transport in the earth's upper mantle. *J. Geophys. Res.* 102 (B11), 24771–24784.
- Vétil, J.Y., Lorand, J.-P., Fabries, J., 1988. Conditions de mise en place des filons des pyroxénites à amphibole du massif ultramafique de Lherz (Ariège, France). *C. R. Acad. Sci. Paris* 307, 587–593.
- Vielzeuf, D., Kornprobst, J., 1984. Crustal splitting and the emplacement of Pyrenean lherzolites and granulites. *Earth Planet. Sci. Lett.* 67, 87–96.
- Walter, M.J., Sisson, T.W., Presnall, D.C., 1995. A mass proportion method for calculating melting reactions and application to melting of model upper mantle lherzolite. *Earth Planet. Sci. Lett.* 135, 77–90.
- Wood, B.J., Blundy, J.D., 2003. Trace element partitioning under crustal and uppermost mantle conditions: the influences of ionic radius, cation charge, pressure, and temperature. In: Carlson, R.W. (Ed.), *Treatise on Geochemistry*. Elsevier, Amsterdam, pp. 395–425.